The 1911 M~6.6 Calaveras earthquake: Source parameters and the role of static, viscoelastic and dynamic Coulomb stress changes imparted by the 1906 San Francisco earthquake

by Diane I. Doser, Kim B. Olsen, Fred F. Pollitz, Ross S. Stein, and Shinji Toda*

Abstract The occurrence of a right-lateral strike-slip earthquake in 1911 is inconsistent with the calculated -0.2 to -2.5 bar static stress decrease imparted by the 1906 rupture at that location on the Calaveras fault, and 5 years of calculated post-1906 viscoelastic rebound does little to reload the Calaveras fault. We have thus used all available first motion, body wave and surface wave data to explore possible focal mechanisms for the 1 July 1911 Calaveras earthquake. We find that the 1911 event was indeed most likely a right-lateral strike-slip event on the Calaveras fault, larger than but otherwise resembling the 1984 M=6.1 Morgan Hill earthquake in roughly the same location. Unfortunately, we could recover no unambiguous surface fault offset or geodetic strain data to corroborate the seismic analysis despite an exhaustive archival search. We calculated the static and dynamic Coulomb stress changes for the three 1906 source models to understand stress transfer to the 1911 site. In contrast to the static stress shadow, the peak dynamic Coulomb stress imparted by the 1906 rupture promoted failure at the site of the 1911 earthquake by 1.4-5.8 bars. Perhaps because the sample is small and the aftershocks are poorly located, we find no correlation of 1906 aftershock frequency or magnitude with the peak dynamic stress, although all aftershocks sustained a calculated a dynamic stress of ≥3 bars. Just 20 km to the south of the 1911 epicenter, we find that surface creep of the Calaveras at Hollister paused for ~17 years after 1906, about the expected delay for the calculated static stress drop imparted by the 1906 earthquake when San Andreas

*Order of authorship is alphabetical; all contributions are equal.

postseismic creep and viscoelastic relaxation are included. Thus, the 1911 Calaveras earthquake may have been promoted by the transient dynamic stresses, while Calaveras creep 20 km to the south appears to have been inhibited by the static stress changes.

Introduction

The 1906 San Francisco earthquake is calculated to have reduced the static stress along adjacent, sub-parallel, strike-slip faults in the greater San Francisco Bay area (Figure 1) (Simpson and Reasenberg, 1994; Harris and Simpson, 1998). Although questioned by Felzer and Brodsky (2005), the 1906 'stress shadow' has been invoked by Simpson and Reasenberg (1994), Harris and Simpson (1998), Stein (1999), and Pollitz et al (2004) to explain the roughly order-of-magnitude drop in the rate of M≥6 shocks in the Bay area in the 75 years following the 1906 earthquake. In contrast to 14 such events in the 75 years preceding 1906, only one M ≥ 6 event, the 1911 Calaveras earthquake, struck in the 75 years after the 1906 earthquake. At least three studies (Jaumé and Sykes, 1996; Harris and Simpson, 1998; Hori and Kaneda, 2001) analyzed why the 1911 earthquake could have occurred in the 1906 stress shadow. Harris and Simpson (1998) and Hori and Kaneda (2001) argued that the 1906 earthquake might have delayed the 1911 event by up to five years, either because it was about to rupture in 1906, or because of the high Calaveras creep rate. Jaumé and Sykes (1996) argued that the 1911 event could have struck on a thrust fault oriented parallel to the Calaveras fault, in which case the 1906 stress changes would be positive, promoting failure. It is thus necessary to determine the focal mechanism, location, and magnitude of the 1911 event, since the sign and magnitude of stress change are dependent on the geometry, location, and rake of the

receiver fault (Simpson and Reasenberg, 1994).

Here we use first motion, regional and teleseismic waveforms of the 1911 event to determine its focal mechanism and improve its magnitude estimation. We then resolve the static and dynamic stress changes imparted by the 1906 shock on the fault plane interpreted from this mechanism. Our conclusions are tempered by the limited low-quality seismic data, but suggest that the event was right-lateral and most likely struck on the Calaveras fault.

Previous Studies

The initial studies of the 1911 Calaveras earthquake summarized mainshock and aftershock arrival times (Wood, 1912a), intensities (Templeton, 1911), earthquake damage and instrumental and human perceptions (Oldenbach, 1911). No reports of surface faulting accompanied the earthquake, although damage reports were later interpreted to indicate a rupture on the Calaveras fault. Gutenberg and Richter (1954) assigned the event a magnitude 6.6 and Ellsworth (1990) an M_S of 6.5.

Oppenheimer et al. (1990) used Wood's travel times to relocate the 1911 aftershocks under the assumption that they occurred along the Calaveras fault, concluding that 1911 aftershocks occurred on same section of the Calaveras fault as the aftershocks of the M=6.1 April 24, 1984 Morgan Hill mainshock. By comparing intensities for the 1984 and 1911 events, Toppozada (1984) concluded that both events had the same magnitude and occurred on overlapping segments of the Calaveras fault. Bakun (1999) reanalyzed the intensity data and found it to be consistent with Calaveras fault rupture in a location similar to that of the 1984 mainshock. He estimated a moment-magnitude of

6.2 (+0.2,-0.3 units) for the mainshock.

Seismic Data

In an attempt to improve the constraints on focal mechanism and magnitude of the 1911 mainshock, we collected first-motion information from instrumental records and from the literature, and obtained all still-extant seismograms for the event. Sadly, nearly all observations from the numerous Jesuit seismic observatories in the United States have been lost. But fortuitously, we were able to obtain seismograms at two stations that recorded both the 1911 and 1984 events. In one case (Göttingen) the seismograms were recorded by instruments that had very similar responses in 1911 and 1984 (Table 1).

Seismic Analysis

First motions

P-waves for the 1911 mainshock were visible only at stations located in central California (Figure 2). The record for the Los Gatos seismoscope (GAT) is published in Oldenbach (1911). First motions for Mt. Hamilton (MHC) and Santa Clara (SCL) were read from copies of the original seismograms. Seismograms at MHC indicated the ground moved down, east and south during the mainshock, contrary to Wood's (1912b) observation that indicated west and north first motions. Ground motion information for Berkeley (BRK) was obtained from Wood (1912b).

Since azimuths and take-off angles for central California stations are sensitive to the event location, we considered two possible event epicenters: a location similar to the Morgan Hill earthquake (37.31 N 121.68 W) (dots, Figure 2) and the intensity center of Bakun (1999) (37.39 N 121.8 W) (stars, Figure 2). Figure 2 compares the first motion

data to the strike-slip mechanism of the 1984 Morgan Hill earthquake (solid lines) and representative normal and reverse focal mechanisms (dashed lines) for earthquakes located just west of the Calaveras fault from Manaker et al. (2005). It appears the data are most consistent with the strike-slip or normal mechanisms, but they are not sufficient to adequately distinguish between mechanisms.

Body waves

Few instruments with sufficient gain to record a magnitude 6.0-6.5 earthquake were operating in the world in 1911. After an extensive search of seismogram archives in the U.S. and requests to seismograph stations operating else in the world, we were able to obtain S waveforms recorded at St. Louis, Missouri (SLM, Δ=25°), Göttingen (GTT, Δ=82°), Debilt (DBN, Δ=80°), and Ottawa (OTT, Δ=35°). In contrast, no S waves were observed at either GTT or DBN for the 1984 Morgan Hill earthquake. We modeled waveforms with the technique of Baker and Doser (1988), modified by Doser and VanDusen (1996). Simple crustal velocity models were used at the source (30-km thick crust with V_p=6.3 km/sec and V_s=3.6 km/sec over a mantle with V_p=8.0 km/sec and V_s=4.2 km/sec) and receivers (35-km thick crust with the same velocities as the source model). The forward modeling indicates that the SH waveform shapes, amplitudes, and polarities match synthetic seismograms for a strike-slip mechanism similar to the 1984 Morgan Hill earthquake (strike=320°, dip=88°, rake=178°) (Figure 3) better than a reverse mechanism (strike=60°, dip=45°, rake=90°) or normal mechanism (strike=30°, dip=30°, rake=-60°) with orientations similar to seismogenic structures observed just west of the Calaveras fault (Manaker et al., 2005). For the strike-slip and reverse mechanisms a starting model with a moment-magnitude of 6.6 best fit the observed

seismograms; however for the normal mechanism a starting model with a moment-magnitude of 6.4 still overpredicted amplitudes observed at European stations (Figure 3).

Surface waves

Figure 4 shows scanned copies of the original surface waveforms recorded at DBN and GTT in 1911 and 1984. The seismograms have been aligned relative to one another based on event travel times. The seismograms at GTT (Figure 4a) were recorded with nearly identical instruments (Table 1). Note the similarities in waveform shape between the two events, although the amplitudes for the 1911 waveforms are a factor of ≤ 5 larger. Waveforms for the 1911 and 1984 earthquakes recorded at DBN also show similar characteristics (Figure 4b), although instrument responses differ (Table 1).

Static Coulomb Stress and Boundary Element Analysis

We calculate that the 1906 earthquake imparted a 2-4 bar left-lateral static shear stress change and a 0.2-2.5-bar drop in Coulomb stress on the Calaveras fault at the site of the future 1911 earthquake. We use the Wald et al (1993), Thatcher et al. (1997), and Song et al (2007) source models for the 1906 earthquake in an elastic half space (Figure 6). The Wald et al. slip model, in part constrained by seismic records from the earthquake, contains a concentration of slip in Sonoma and southern Mendocino Counties as well as on the San Francisco Peninsula and into southern Marin County toward the North (Figure 6). In contrast, the Thatcher et al. and Song et al. models are smoother, with significant slip from Point Arena to the North and Hollister to the South. The geodetic data used in the Thatcher et al and Song et al models require greater 1906 slip on the San Andreas near the 1911 epicenter than in the Wald et al model, making them more

reliable for Calaveras calculations. The slip profiles shown in Figure 6 were extended to the bottom of the vertical fault plane (12 km for the Wald et al. and Song et al. models, and 10 km for the Thatcher et al. model). The Thatcher et al. (-1.9 bars) and Song et al. (2.5bars) models yield the largest decreases; the Wald et al. model (-0.2 bars) is the smallest (Figure 5). Harris and Simpson (1998) calculated a 2.0-bar stress change, and most studies find measurable seismicity responses to stress changes exceeding 0.1 bars (Stein, 1999). Hollister, whose 100-year surface creep record is used for this study, has static Coulomb stress drop of 5.8 bars for Thatcher et al., 6.6 bars for Song et al., and 2.3 bars for the Wald et al.

Estimating the earthquake delay caused by the 1906 stress shadow

We next performed a boundary element analysis to estimate the amount of tectonic stress accumulation that would be needed to shed the 0.2 to 2.5-bar stress imposed by the 1906 earthquake. Here we treat the Calaveras fault as a 15-km deep surface of freely slipping boundary elements, in a manner similar to Toda and Stein (2002). The amount of stress depends not just on the magnitude of the stress change at the 1911 site and the longterm slip rate, but also on the geometry and distribution of stresses along the entire fault, since the longer and straighter the fault, the more it will slip in response to a given change in stress. We find that 350±50 mm of left-lateral slip (also known as 'back-slip') would be needed to relieve the imposed stress (Figure 7). Given the long-term 15±3 mm/yr slip rate on this section of the Calaveras (U.S. Geological Survey, 2007), the slip deficit would be removed in 23.3±0.25 years. Instead, the 1911 earthquake struck after just 5 years, long before the stress drop imparted by the 1906 shock is likely to have been erased by stress

accumulation.

The ratio of the 1906 stress drop on the Calaveras fault to the long term stressing rate of the Calaveras furnishes a complementary way to estimate the expected delay of M~6 Calaveras earthquakes. The stressing rate is influenced by the stress contribution from other faults within about 30 km of the 1911 site (e.g., 2-3 fault depths), such as the southern Hayward and San Andreas. So we used an interseismic stressing model in which locked faults are treated as virtual dislocations (they are slipped backwards at their long term rates) over their locked width in an elastic half space. We then sample the average stressing rate on the 1911 site on the Calaveras fault over 0-10 km depth (the 1984 Morgan Hill mainshock nucleated at 8 km depth), and find the Calaveras stressing rate at the site of the 1911 shock to be 0.15±0.05 bars/yr, the value used by Harris and Simpson (1998). In comparison, Pollitz et al (2004) and Parsons (2006) used 0.09 bars/yr for the Calaveras fault in the absence of creep. The expected delay using our stressing rate then comes to 27±9 yr, in agreement with the boundary element calculation.

A third way to estimate the delay is to consider the 1911 and 1984 earthquakes as ruptures of the same fault patch. In the absence of the stress changes imparted to the Calaveras by the 1906 shock, given the 15±3 mm/yr Calaveras slip rate the period between 1911 and 1984 would nominally accumulate a 1.1±0.2 m slip deficit. A strike-slip Mw=6.5 shock has a typical slip of 1.0 m and a rupture area of 10 x 30 km (Wells and Coppersmith, 1994). The 1911 aftershock zone as relocated by Oppenheimer et al. (1990) is about 20 km long, and aftershocks of the 1984 Morgan Hill shock extended for ~28 km, with slip occurring over a patchy region of total area 27 x 11 km (Oppenheimer et al., 1990), in fair agreement with the magnitude estimate provided by our seismic

analysis assuming a 3 x10^{11} dyne-cm^2 shear modulus. Thus, a minimum inter-event time of 73 years for the 1911 event is needed to re-accumulate sufficient stress for another M~6 shock. If one assumes that the 1911 and 1984 events have typical 30-bar stress drops, then a 4-bar stress drop in 1906 represents about 15% of the total, which would have erased at least 10 yrs of stress accumulation, providing a lower bound on the other estimates we have made. But the 1911 and 1984 shocks could have slipped adjacent or complementary patches of the fault, as occurred during the 1934, 1966, and 2004 Parkfield shocks (Segall and Du, 1993; Murray and Langbein, 2006), in which case the inter-event time for the 1911 event could be much longer than 73 years, and the retardation could similarly be much longer than 10 years.

Dynamic Coulomb stress analysis

While the static Coulomb Failure Function (static-CFF) for numerous earthquakes has been successfully correlated with aftershocks and subsequent mainshocks, Kilb et al. (2002) and Kilb (2003) proposed an alternative parameter to estimate seismic triggering potential, the peak dynamic-CFF change, which is highly sensitive to rupture effects such as directivity. They illustrated this sensitivity by an improved correlation of peak dynamic-CFF with aftershocks for the M=7.3 Landers, CA, earthquake, as compared to static-CFF estimates. In contrast, static-CFF estimates are primarily sensitive to the slip distribution and geometry of the rupture surface.

Here we compare the peak dynamic Coulomb stress changes for the three source models of the 1906 earthquake (Figure 8). Although Thatcher et al (1997) presented a static displacement model, we use it to generate a kinematic rupture model by assuming

an epicenter 10 km south of the Golden Gate off Daly City, and a uniform rupture velocity of 2.7 km/sec (as used by Wald et al. (1993) for their rupture model of the 1906 event, based on studies of other California strike-slip earthquakes). The Coulomb stress changes were computed at 8 km depth in a layered regional model within a 630 km by 260 km area using a fourth-order finite difference method (Olsen, 1994), a friction coefficient of 0.4 (Stein, 1999) and resolved on to vertical faults parallel to the local strike of the Calaveras fault (144^{o}). Reducing the friction to 0.2 has little effect (Figure 9). The Wald et al. and Thatcher et al. source models were implemented using a constant (sub-shear) rupture velocity of 2.7 km/s, as used in the teleseismic modeling of Wald's study. The Song et al. model, on the other hand, used four different rupture velocities along the fault, with a super-shear segment located near the epicenter.

The peak dynamic-CFF distributions shown in Figure 8 for the three source models reveal more strikingly different patterns. Unlike the static-CFF, the peak dynamic-CFF are everywhere positive, and contain significant effects of the rupture propagation, as pointed out by Kilb (2003), with a strong directivity pattern. The most prominent directivity effects occur for the relatively large slip in the Thatcher et al. and Song et al. models toward the north. In contrast, the peak dynamic-CFF values are relatively modest in the epicentral area. The Song et al. model contains smaller peak dynamic-CFF values near the epicenter, to a large extent an effect of the super-shear rupture velocity in this area. At the site of the 1911 earthquake, the peak dynamic-CFF predicted by the Wald et al., Thatcher et al. and Song et al. Models reach ~1 bar, 6 bars and 6 bars, respectively. The San Andreas at Hollister is calculated to have sustained a peak dynamic-CFF of 2 bars for the Wald et al. 1906 model and 10 bars for both Thatcher

et al. and Song et al. Since the fault is creeping at this locality, it might have been expected to undergo accelerated creep rather than the observed creep pause.

The 1911 earthquake could have been triggered by dynamic Coulomb stresses. In addition to our calculations for the site of the Calaveras shock, we note that the five aftershocks that occurred between the 1906 mainshock and the 1911 earthquake (Meltzner and Wald, 2003) all stuck where the dynamic Coulomb stress exceeded 3 bars (Figure 12). Nevertheless, this test is less stringent than for the static stress change since the peak dynamic stress changes are positive, whereas static stress changes are both positive and negative. Further, aftershocks were not recorded—or did not occur—in many of the regions with the highest peak dynamic stress changes, and as a result there is no correlation between peak dynamic Coulomb stress and either aftershock frequency or magnitude (Figure 12). The absence of a correlation may be the product of the impoverished aftershock catalog.

Discussion

Inferences on the 1911 rupture propagation direction

The limited seismic data suggest that the mechanism of the 1911 earthquake may be consistent with right-lateral rupture along the Calaveras fault, similar to the 1984 M=6.1 Morgan Hill earthquake. However, the lack of S-waves at teleseismic distances for the Morgan Hill earthquake and the smaller amplitude of its surface waves as recorded at GTT suggest that the 1911 earthquake had a greater magnitude ($6.3 \geq M \geq 6.6$), its direction of rupture propagation was different than the 1984 event, or the data are

suspect. Since both GTT and DBN are located along strike to the northwest of the epicenter (Figure 3), unilateral rupture to the southeast in 1984 (Bakun et al., 1984) and toward the northwest in 1911 might explain some of the amplitude differences between seismograms.

Search for historical evidence of 1906 or 1911 Calaveras slip

To learn if the Calaveras fault slipped in response to the 1906 earthquake, we searched for evidence of surface slip or deformation. We searched for astronomic-azimuth measurements that might have been carried out by the Lick Observatory to align its telescope at Mt. Hamilton, which is located 5-10 km north of the 1911 epicenter. We also looked for cultural-offset or geological observations from the contemporary literature, including newspaper accounts of ruptured conduits or offset railways, road or fences, and cadastral surveying measurements for property boundaries. A Southern Pacific railway line crosses the fault obliquely 2.5 km north of Hollister, but no archives of rail repairs from this period exist. The April 20, 1906 edition of the Hollister newspaper reported that "The big water main on Fifth Street was torn heavily apart, and but for the prompt action of the water company, the town would have been without water." (The Free Lance, 1906). The Calaveras fault traverses Fifth Street between Powell and West Streets (Rogers and Nason, 1971), but where on Fifth the water main was ruptured was not reported. The water main is likely to have been a buried cast iron pipe, and so fault offset is possible but equivocal. E. C. Templeton reported that at the time of the 1911 shock, "the earthquake cracked the loose gravels at the side of the stream…At one house near here, the most serious damage was the disconnecting of a

water pipe at a windmill" on the Coyote Creek 2 km northeast of Edenvale, near the Calaveras fault (Oldenbach, 1911). Although this could be associated with coseismic 1911 slip, it is ambiguous.

Post-1906 creep retardation at Hollister

Unlike the 1911 site, there are surface slip measurements ~20 km to the southeast at Hollister beginning in 1909 (Figure 1b). This reveals a likely 17-year pause in surface creep following the 1906 earthquake, with no change in 1911 (Figure 10). A boundary element calculation using the Thatcher et al (1997) model indicates that at Hollister, 0.7 m of left-lateral slip, or a pause in right-lateral creep equivalent to 0.7 m, would have shed the 5 bars of left-lateral stress imposed in 1906 (Figure 7). If the creeping section of the San Andreas fault extending southeast from Hollister slipped postseismically to relieve the 1906-imposed changes, the Calaveras stress drop would reduce to 2.2 bars, and the resulting left-lateral slip needed to relieve the imposed stresses would be 0.5 m (Figure 7). Given the observed 15±3 mm/yr slip rate at Hollister (6.8 mm/yr of which occurs as surface creep) and the 0.5-0.7 m of back slip, a 33-47 yr pause in Hollister creep would be expected, at least twice as long as the observed pause.

Impact of viscoelastic relaxation on Calaveras earthquakes and creep

Viscoelastic relaxation speeds the re-stressing of the Calaveras fault, and thus could contribute to the shortened creep retardation at Hollister, in comparison to purely elastic models. However, viscoelastic recovery does not significantly reload the site of the 1911 earthquake during the 5 years after the 1906 earthquake. Following a 5-bar 1906

stress drop, the stress recovery during the ensuing 5 years at the 1911 epicenter is calculated to be just 0.15 bars using the model of Pollitz et al. (2004) (Figure 11a). In contrast, at the Hollister site viscoelastic rebound is calculated to reach 1.0 bars by 1916, and 2.0 bars by 1926 (Figure 11b). This stress recovery approximately matches the observed delay in Hollister creep (Figure 10).

Other explanations for the occurrence of the 1911 shock

Harris and Simpson (1998) invoked rate/state friction of Dieterich (1994) to explain the occurrence of the 1911 earthquake. They posited that if in the absence of the 1906 earthquake that section of the Calaveras fault would have ruptured in 1908, then the 1906 stress shadow could have delayed the event by only 5 years. This arises because in rate/state friction theory, a given stress change has a more modest effect in delaying or advancing the rupture late in an earthquake cycle (Dieterich, 1994). While an intriguing hypothesis, it is unfortunately untestable, because the unperturbed failure time of the Calaveras patch cannot be known. Hori and Kaneda (2001) supposed that because of fault creep, the stressing rate surrounding the locked 1911 patch could be as high as 1-2 bar/yr—much higher than our two independent estimates—in which case the 1906 stress decrease would have been erased in several years, making the 1911 event more likely. The 17-year delay at Hollister makes the Hori and Kaneda (2001) explanation for the occurrence of the 1911 earthquake less tenable, because the Hollister creep pause should have also been very brief if the stressing rate were in fact as high as 1-2 bars/yr.

Conclusions

First motion, body wave and teleseismic surface wave analysis for the first time permits a focal mechanism analysis of the 1911 Calaveras earthquake. We find that it was most likely a M~6.5 right-lateral event on the Calaveras fault. Our mechanism, location, and magnitude are consistent with assumptions made by Oppenheimer et al. (1990), Harris and Simpson (1998), and Bakun (1999), but inconsistent with Jaumé and Sykes (1996), who suggested that it was a reverse mechanism located east of the Calaveras fault, and likely inconsistent with Hori and Kaneda (2001), who proposed a fault stressing rate that is too high to explain the Hollister creep pause. The mechanism and location of the 1911 shock means that it struck on a fault in the stress shadow of the 1906 earthquake, and thus cannot be easily reconciled with the static Coulomb stress hypothesis.

The 1911 earthquake occurred only about a quarter-way through an expected retardation of about 25 yr caused by the 1906 earthquake, and viscoelastic re-stressing would have only shortened this by a small amount. Thus, the best explanation for the occurrence of the 1911 shock is that it was promoted by the peak dynamic Coulomb stress imparted by the 1906 earthquake. Nevertheless there are not enough well-located aftershocks to be confident in this assessment.

We also find that creep retardation occurred at Hollister, just 20 km to the southeast on the Calaveras fault, which also lies in the stress shadow of the 1906 earthquake. The 17-yr creep retardation can be fully explained by the coseismic stress drop, postseismic San Andreas creep, and viscoelastic recovery. Thus the creep retardation provides evidence in support of the static Coulomb hypothesis. In contrast, the San Andreas at Hollister is calculated to have experienced a peak dynamic-CFF of 6-10

bars and thus if creep were also driven by dynamic stresses above 3 bars, the creep should have accelerated rather than paused.

Acknowledgments. We thank reviewers Steve Jaumé and Debi Kilb, and David Oppenheimer for comments that greatly improved the manuscript. We also thank Elliot Grunewald, Lee Rosenberg, Willie Lee, John Ebel, and Steve Jaumé for their assistance in locating seismograms and other historical information. We would also like to thank seismograph station managers around the world who maintain and helped us recover the 1911 and 1984 seismograms.

References

Baker, M.R., and D.I. Doser (1988). Joint inversion of regional and teleseismic earthquakes waveforms, J. Geophys. Res. 93, 2037-2045.

Bakun, W.H., (1999). Seismic activity of the San Francisco Bay region, Bull. Seismol. Soc. Amer. 89, 764-784.

Bakun, W.H., M.M Clark, R.S. Cockerham, W.L. Ellsworth, A.G. Lindh, W.H. Prescott, A.F. Shakal, and P. Spudich (1984). The 1984 Morgan Hill, California, earthquake, Science, 225, 228-291.

Dieterich, J., (1994). A constitutive law for rate of earthquake production and its application to earthquake clustering, *J. Geophys. Res.*, *99*, 2601-2618.

Doser, D.I., and S.R. VanDusen (1996). Source processes of large (M≥6.5) earthquakes of the southeastern Caribbean (1926-1960), Pure Appl. Geophys. 146, 43-66.

Ellsworth, W.L. (1990). Earthquake history, 1769-1989, The San Andreas Fault System, California, R.E. Wallace (Editor), Chap. 6, U.S. Geol. Surv. Profess. Pap. 151, 153-188.

Felzer, K.R. and E.E. Brodsky (2005). Testing the stress shadow hypothesis, J. Geophys. Res. 110, doi:10.1029/2004JB003277.

Felzer, K.R., and T. Cao (2008). WGCEP Historical California earthquake catalog,

Appendix H in The Uniform California Earthquake Rupture Forecast, version 2 (UCERF 2): U.S. Geological Survey Open-File Report 2007-1437H and California Geological Survey Special Report 203H, 127 p. [http://pubs.usgs.gov/of/2007/1437/h/] Gutenberg, B., and C.F. Richter (1954). Seismicity of the Earth and Associated Phenomena, 2nd ed., Princeton University Press, Princeton, New Jersey, 310 pp.

Harris, R.A., and R.W. Simpson (1998). Suppression of large earthquakes by stress shadows: A comparison of Coulomb and rate-and-state failure, J. Geophys. Res. 103, 24,439-24,451.

Hori, T., and Y. Kaneda (2001). A simple explanation for the occurrence of the 1911 Morgan Hill earthquake in the stress shadow of the 1906 San Francisco earthquake, Geophys. Res. Lett. 28, doi:10.1029/2000GL012727.

Jaumé, S.C., and L. R. Sykes (1996). Evolution of moderate seismicity in the San Francisco Bay region, 1950 to 1993: Seismicity changes related to the occurrence of large and great earthquakes, J. Geophys. Res. 101, 765-789.

Kilb, D., J. Gomberg, and P. Bodin (2002). Aftershock triggering by complete Coulomb stress changes, J. Geophys. Res., 107, doi:10.1029/2001JB000202.

Kilb, D. (2003). A strong correlation between induced peak dynamic Coulomb stress change from the 1992 *M*7.3 Landers, California, earthquake and the hypocenter of the 1999 *M*7.1 Hector Mine, California, earthquake, J. Geophys. Res.108, doi:10.1029/2001JB000678.

Manaker, D.M., A.J. Michael and R. Burgmann (2005). Subsurface structure and kinematics of the Calaveras-Hayward fault stepover from three-dimensional V_p and seismicity, San Francisco Bay region, California, Bull. Seismol. Soc. Amer. 95, 446-470.

Meltzner, A.J., and D.J. Wald, (2003). Aftershocks and Triggered Events of the Great 1906 California Earthquake, Bull. Seismol. Soc. Amer. 93, 2160–2186., 2003.

Murray, J., and J. Langbein (2006). Slip on the San Andreas Fault at Parkfield, California, over Two Earthquake Cycles, and the Implications for Seismic Hazard, Bull. Seismol. Soc. Amer. 96, S283–S303.

Oldenbach, F.L. (1911). Notes on the California earthquake of July 1, 1911, Bull. Seismol. Soc. Am. 1, 110-121.

Oppenheimer, D.H., W.H. Bakun, and A.G. Lindh (1990). Slip partitioning of the Calaveras fault, California, and prospects for future earthquakes, J. Geophys. Res. 95, 8483-8498.

Olsen, K.B. (1994). Simulation of three-dimensional wave propagation in the Salt Lake Basin, University of Utah (PhD thesis).

Parsons, T., Tectonic stressing in California modeled from GPS observations, J. Geophys. Res., 111, B03407, doi:10.1029/2005JB003946, 2006.

Pollitz, F., W.H. Bakun and M. Nyst (2004). A physical model for strain accumulation in the San Francisco Bay region; stress evolution since 1838, J. Geophys. Res. 109, doi:10.1029/2004JB003003.

Rogers, T.H., and R.D. Nason (1971). Active displacement on the Calaveras fault zone at Hollister, California, Bull. Seismol. Soc. Am. 61, 399-416.

Segall, P., and Y. Du (1993). How similar were the 1934 and 1966 Parkfield earthquakes?, J. Geophys. Res., 98, 4527–4538.

Simpson, R. W. and P. A. Reasenberg, Earthquake-induced static-stress changes on central California faults, U.S. Geol. Surv. Prof. Pap. 1550-F, 55-89, 1994.

Song, S.-G., Gregory C. Beroza, G.C., and P. Segall (2007). A unified source model for the 1906 San Francisco earthquake, Bull. Seismol. Soc. Amer., in press.

Stein, R.S., (1999). The role of stress transfer in earthquake occurrence, Nature 402, 605-609.

Templeton, E.C. (1911). The central California earthquake of July 1, 1911, Bull. Seismol. Soc. Am. 1, 167-169.

Thatcher, W., Marshall, G., and M. Lisowski (1997). Resolution of fault slip along the 470-km-long rupture of the great 1906 San Francisco earthquake and its implications, J. Geophys. Res. 102, 5,353-5,367.

The Free Lance (1906). Earthquake! Havoc and destruction wrought in a few seconds; Hollister's loss is $250,000, Hollister, Calif. newspaper, vol. XXIII, No. 16, 20 April 1906.

Toda, S., and R. S. Stein (2002). Response of the San Andreas Fault to the 1983 Coalinga-Nuñez Earthquakes: An Application of Interaction-based Probabilities for Parkfield, J. Geophys. Res. 107, 10.1029/2001JB000172.

Toppozada, T.R. (1984). History of earthquake damage in Santa Clara County and comparison of 1911 and 1984 earthquakes, in The 1984 Morgan Hill, California Earthquake, J.H. Bennett and R.W. Sherburne (Editors), Calif. Div. Mines Geol. Spec. Publ. 68, 237-248.

Wald, D.J., H. Kanamori, D.V. Helmberger, and T.H. Heaton (1993). Source study of the 1906 San Francisco earthquake, Bull. Seismol. Soc. Am. 83, 981-1019.

Wells, D.L., and K.J. Coppersmith (1994). New empirical relationships among magnitude, rupture length, rupture width, rupture area, and surface displacement, Bull. Seismol. Soc. Am. 84, 974-1002.

Wood, H.O (1912a). On the region of origin of the central Californian earthquakes of July, August and September, 1911, Bull. Seismol. Soc. Am. 2, 31-39.

Wood, H.O. (1912b). The registration of earthquakes at the Berkeley station from April 1 to September 30, 1911 and at the Lick Observatory station from May 23 to September 30, 1911, Bull. Of the Seismographic Stations No. 2, Univ. of Calif. Publications, 11-48.

U.S. Geological Survey (2007). California Reference Geologic Fault Parameter Database, compiled by the USGS, CGS, SCEC Working Group for California Earthquake Probabilities,(http://gravity.usc.edu/WGCEP/resources/data/refFaultParams/index.html), U.S. Geol. Surv. Open-File Rep., submitted.

Wald, D.J., Kanamori, H., Helmberger, D.V., and T.H. Heaton (1993), Source Study of the 1906 San Francisco Earthquake, Bull. Seism. Soc. Am. 83, 981-1019.

Department of Geological Sciences
University of Texas at El Paso
El Paso, TX 79968
(D.I.D.)

U.S. Geological Survey
345 Middlefield Road, MS 977
Menlo Park, CA 94025
(R.S.S.; F.P.)

Geological Survey of Japan
Advanced Institute of Science and Technology
Higashi 1-1
Tsukuba 305-8567, Japan
(S.T.)

Department of Geological Sciences
San Diego State University, MC1020
San Diego, CA 92182-1020
(K.B.O.)

Table 1 – Instrument Response Information

Instrument	Seismometer period (sec)	Damping	Magnification
GTT NS (1911) astatic pendulum	12.2	4	160
GTT EW (1911) astatic pendulum	12.2	3.5	159
GTT NS (1984) astatic pendulum	9.4	2.8	153
GTT EW (1984) astatic pendulum	10.3	3.5	157
DBN EW (1911) Wiechert	5	4	170
DBN NS (1911) Wiechert	5	4	170
DBN EW (1984) Galitzin	25	---	310
DBN NS (1984) Galitzin	25	---	310
OTT NS (1911) Bosch	5.6	8	120
OTT EW (1911) Bosch	8	8	120

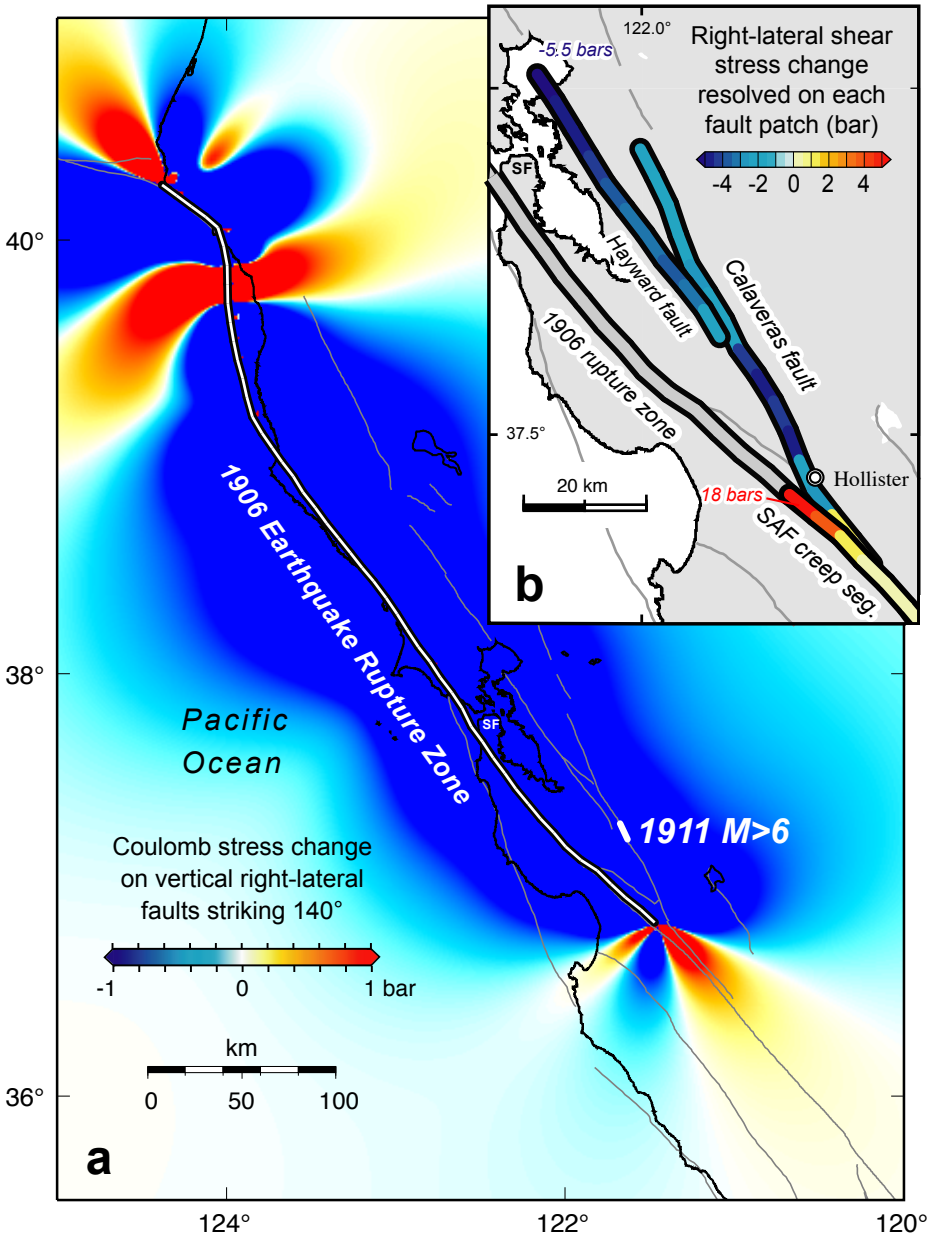

Figure 1 – (a) Map showing static Coulomb stress change imparted by the 1906 earthquake (using the coseismic slip model of Thatcher et al, 1997) on vertical right-lateral strike slip faults striking 140°, the average northern San Andreas strike. (b) Right-lateral shear stress change resolved on the local strike of the Hayward, Calaveras faults, and creeping segment of the San Andreas fault (SAF).

Fig. 1
Doser et al
25 Aug 08

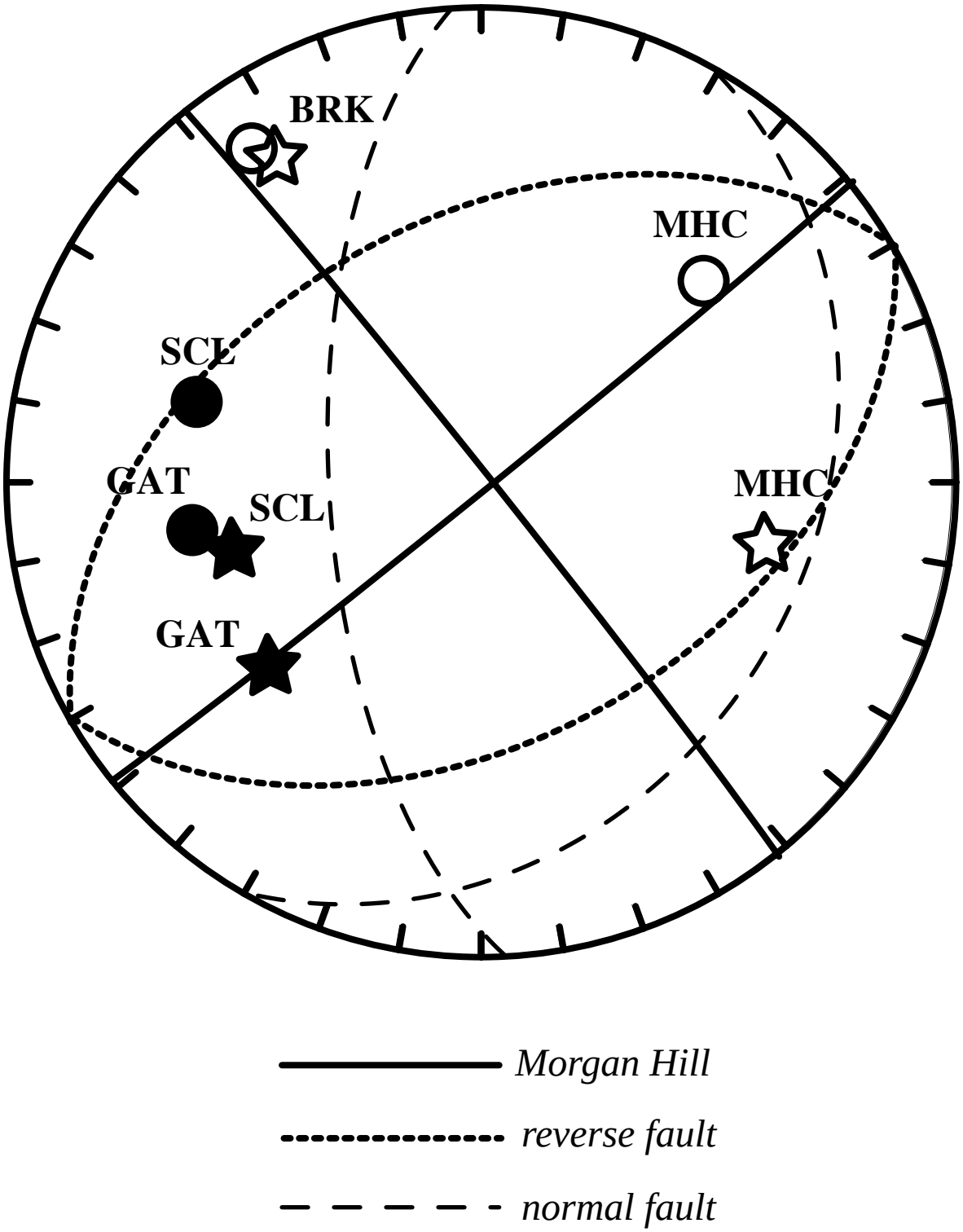

Figure 2 – First motions observed for the 1911 Calaveras earthquake. Open symbols are dilatations, solid symbols are compressions. Dots indicate azimuth and take-off angle positions using 1984 Morgan Hill epicenter, stars indicate positions using Bakun's (1999) intensity center. Focal mechanisms shown are for the Morgan Hill earthquake (solid lines) and representative normal and reverse mechanisms (dashed and dotted lines) for earthquakes occurring in this region of the Calaveras fault (Manaker et al., 2005).

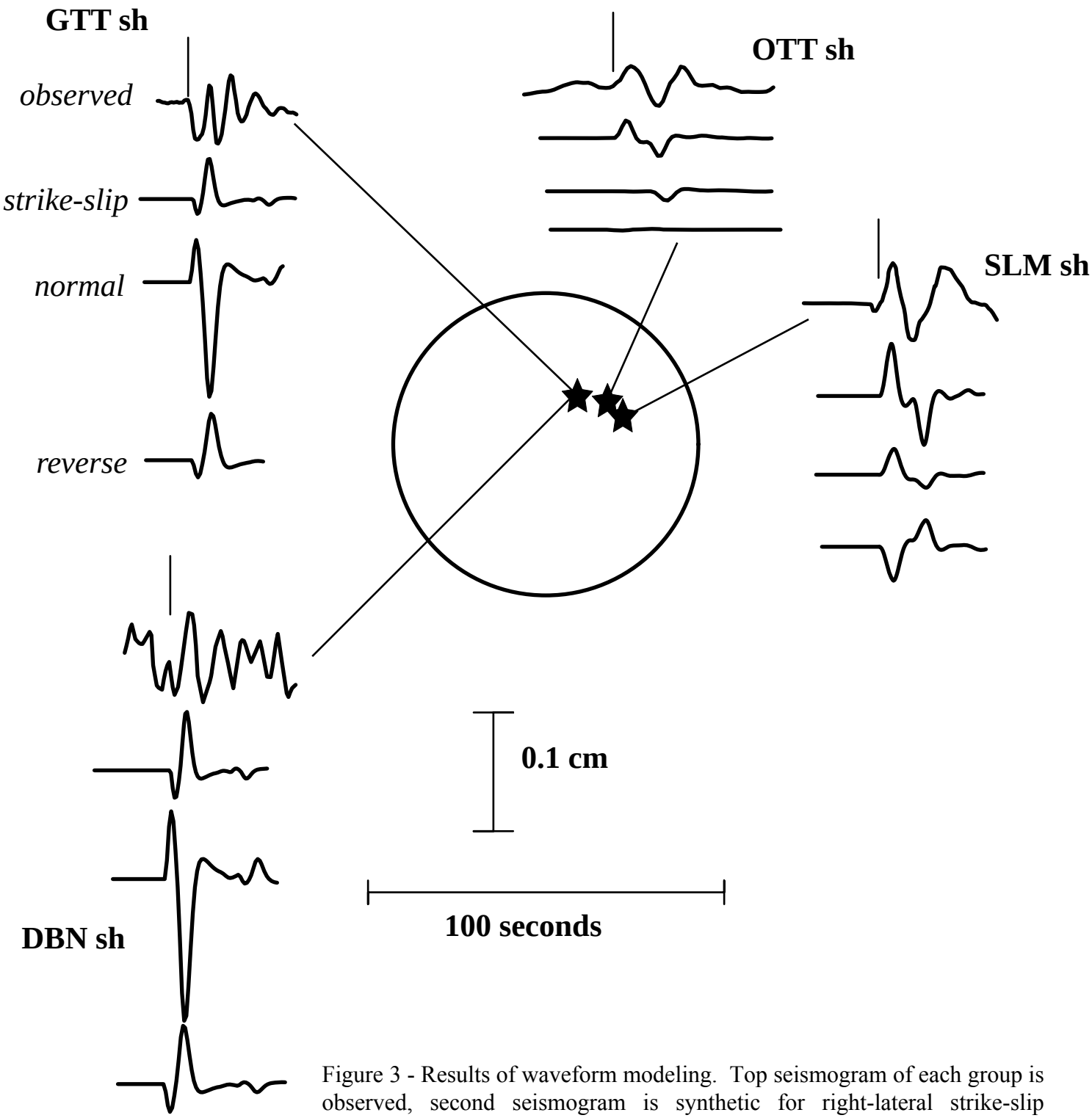

Figure 3 - Results of waveform modeling. Top seismogram of each group is observed, second seismogram is synthetic for right-lateral strike-slip mechanism similar to 1984 Morgan Hill earthquake, third seismogram is synthetic for normal mechanism, fourth seismogram is synthetic for reverse mechanism (see text for details). Solid vertical lines indicate beginning of SH phase on observed seismogram.

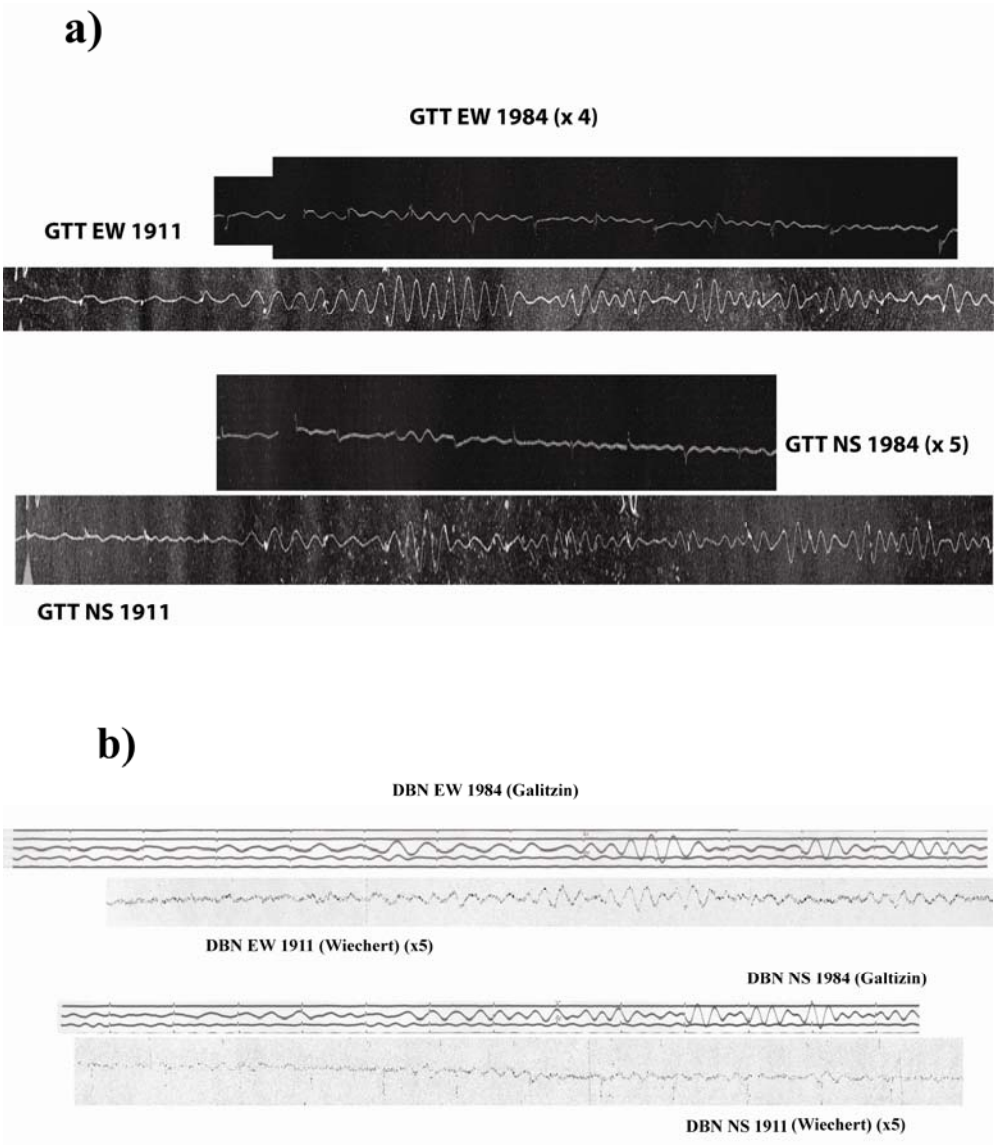

Figure 4 - Comparison of surface waves recorded at GTT (a) and DBN (b) from scanned copies of the original seismograms. Seismograms are aligned with each other based earthquake on travel times. Horizontal scales have been adjusted so that seismograms have the same time scale. For visibility the 1984 seismograms at GTT have been enlarged

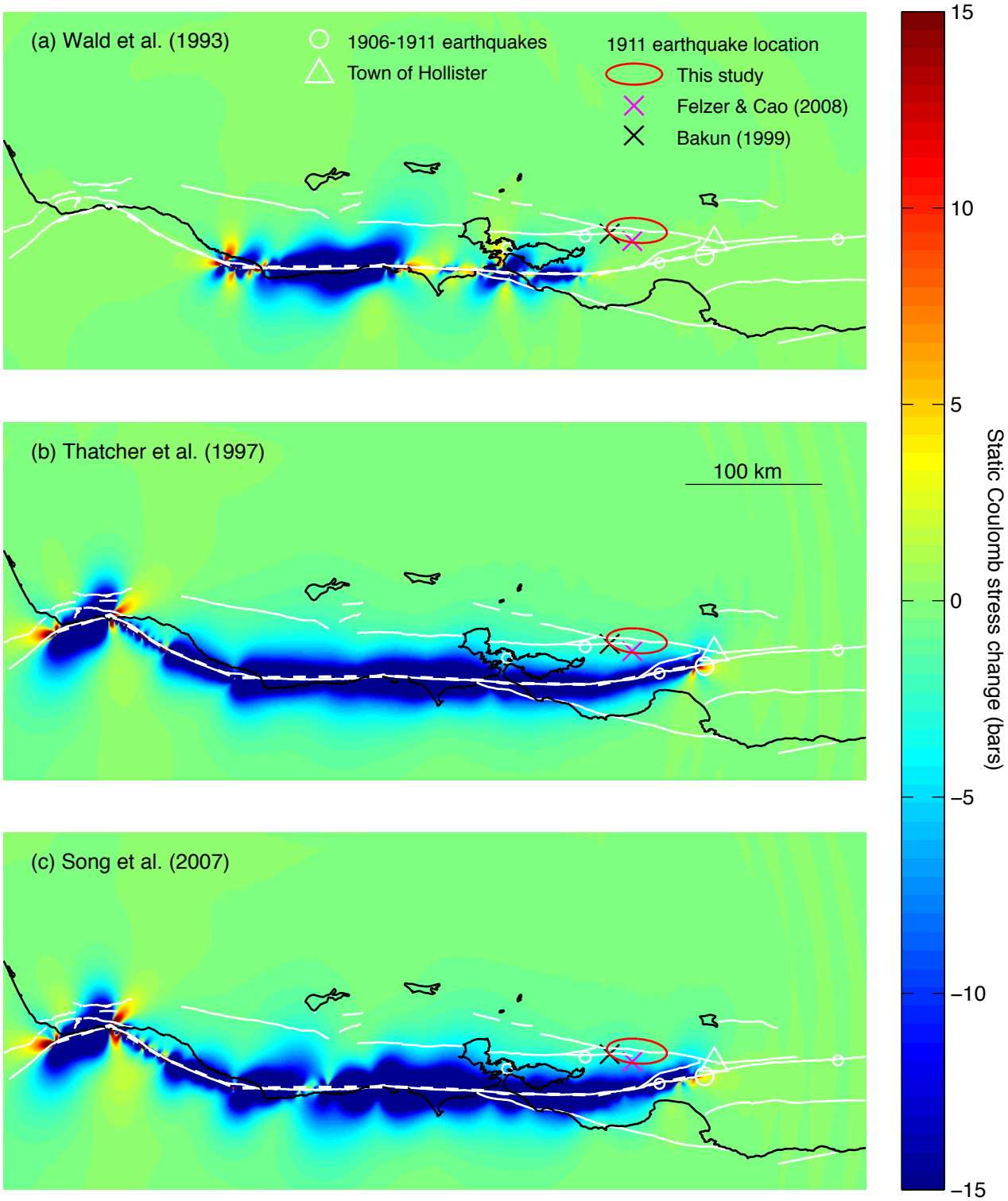

Figure 5 – The static Coulomb stress at 8 km depth imparted by the 1906 quake using slip models by (a) Wald et al. (1993), (b) Thatcher et al. (1997), and (c) Song et al. (2006), assuming a 0.4 friction coefficient on vertical receiver faults striking 144°. Circle size is proportional to magnitude for 1906-1911 aftershocks from Meltzner and Wald (2003).

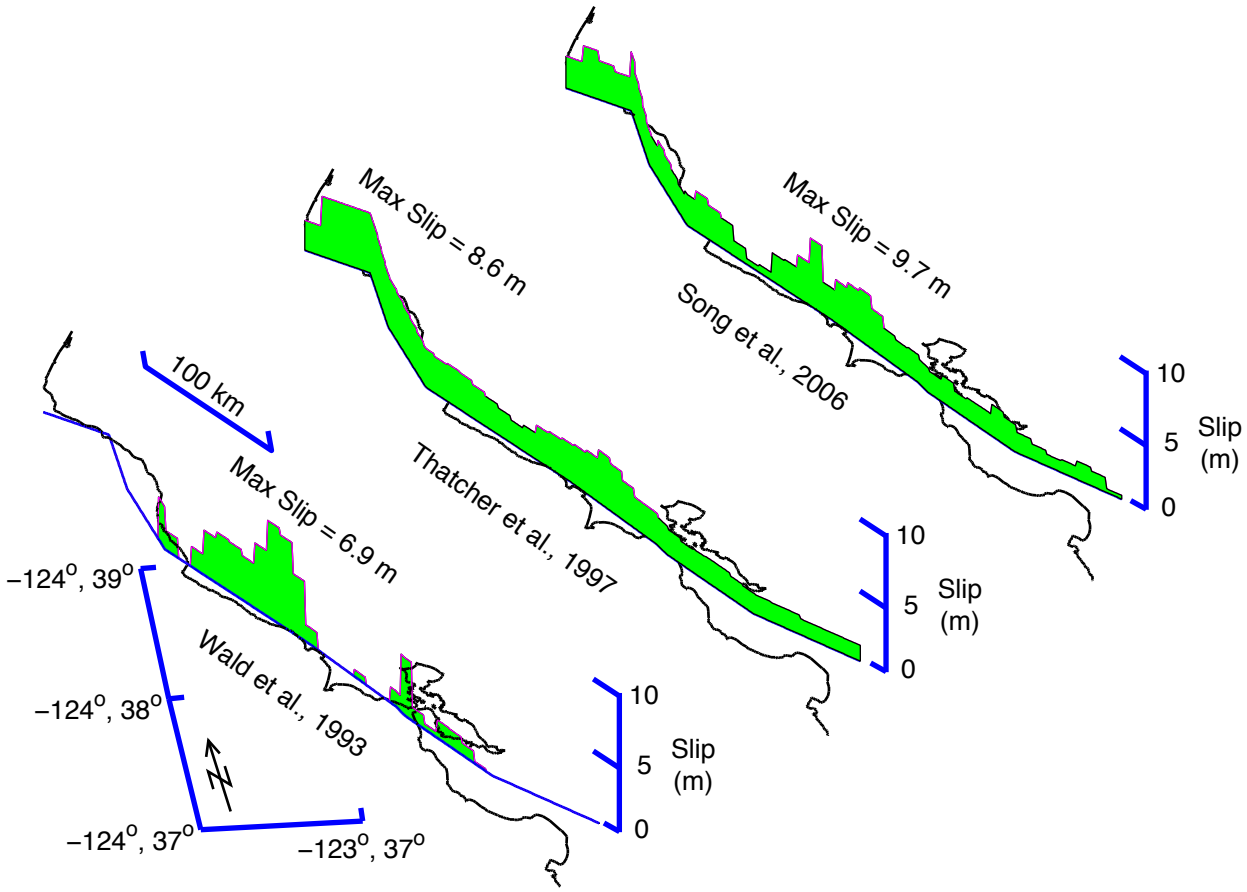

Figure 6 – Comparison between the slip models for the 1906 event by Wald et al. (1993), Thatcher et al. (1997) and Song et al. (2006).

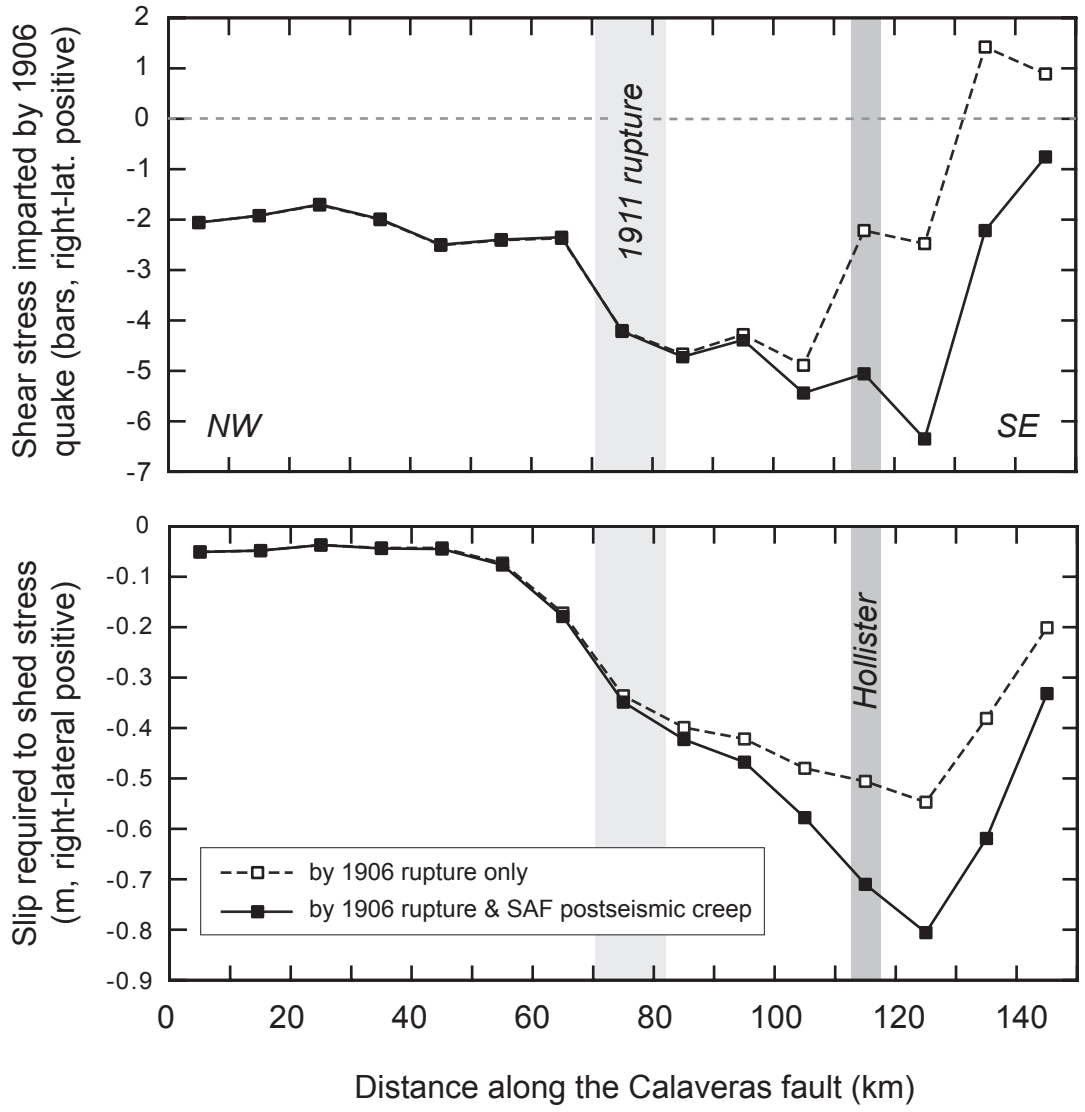

Figure 7 – (a) Shear stress imposed by 1906 earthquake on the Calaveras fault, using the Thatcher et al (1997) slip model; the shear stress changes are also shown by colors in Figure 1b. (b) Slip required to shed (or remove) the stress imposed by 1906 earthquake

Fig. 7
Doser et al
25 Aug 08

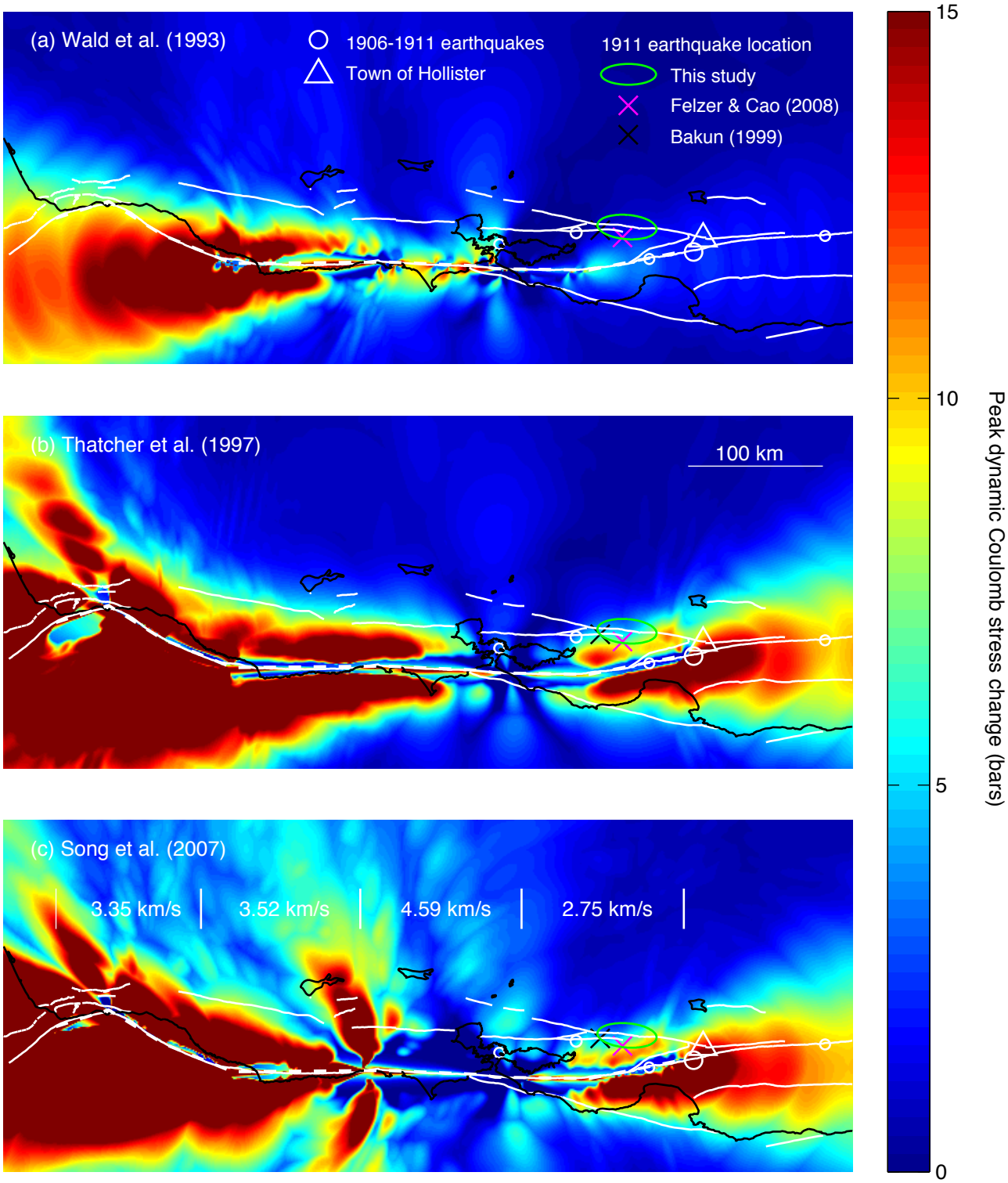

Figure 8 – Peak dynamic Coulomb stress distributions generated by the (a) Wald et al. (1993), (b) Thatcher et al. (1997), and (c) Song et al. (2006) source models. Circle size is proportional to magnitude for 1906-1911 aftershocks from Meltzner and Wald (2003) . The spatially-variable rupture speed is shown for each model. Receiver fault friction is assumed to be 0.4, and symbols are as in Figure 5. Note that the stress scale ranges over 0-15 bars; blue does not represent a stress decrease as it does in Figure 6.

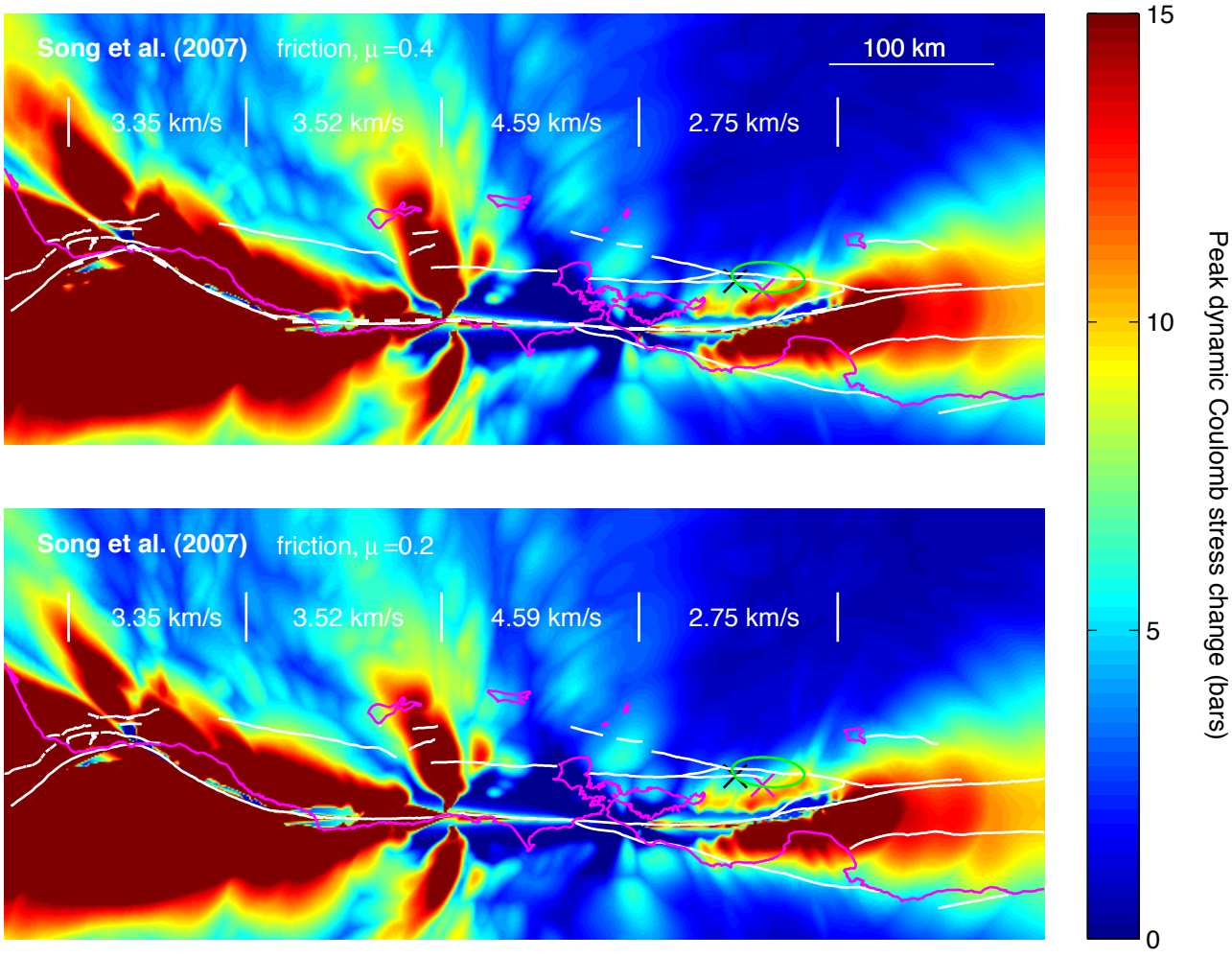

Figure 9. The effect on the peak dynamic Coulomb stress of lowering the assumed friction coefficient on receiver faults from 0.6 (Figure 8) to 0.4 to 0.2 here is modest.

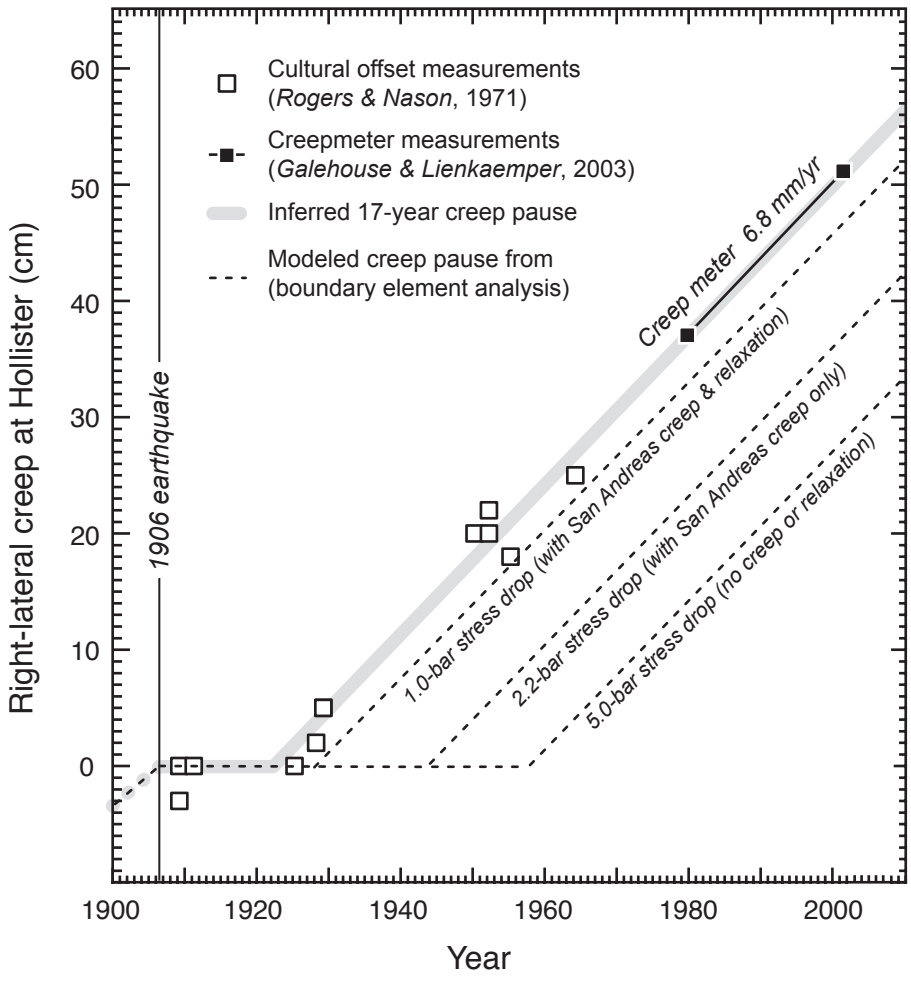

Figure 10 – Creep observations (boxes and solid black line) at Hollister since 1910 compared to stress relaxation models. Thick gray line indicates inferred 17-year creep pause and dashed black lines indicate creep retardation models for 2-5-bar stress drop in 1906.

Fig. 10
Doser et al
25 Aug 08

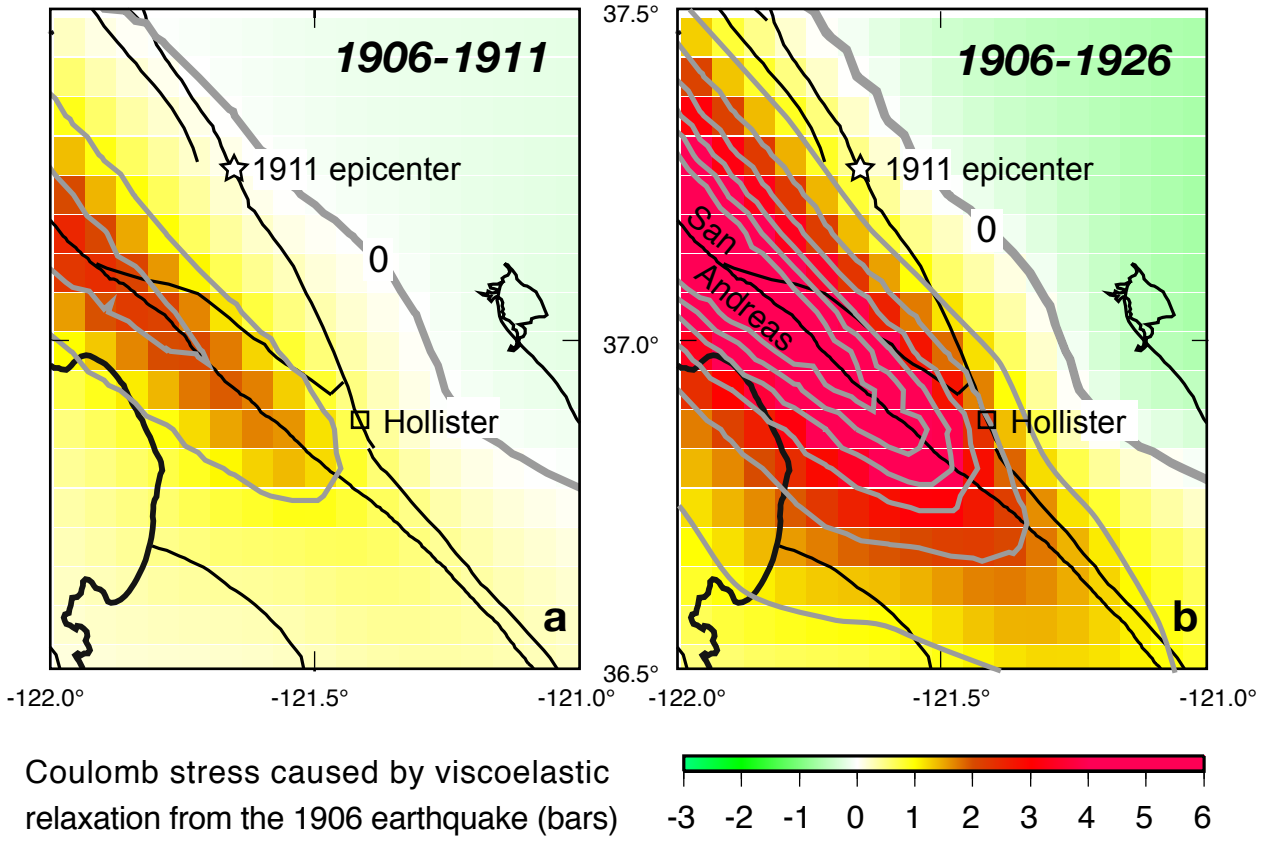

Figure 11. Modeled reloading of fault stress caused by viscoelastic relaxation associated with the 1906 earthquake. (a) At the time of the 1911 earthquake, the Calaveras fault stress has only increased by 0.2 bars. (b) Within several years of the end of the observed creep pause at Hollister , the Calaveras fault has recovered 2.0 bars of Coulomb stress.Longterm or 'secular' stress loading is not included in this calculation.

Fig. 11
Doser et al
25 Aug 08

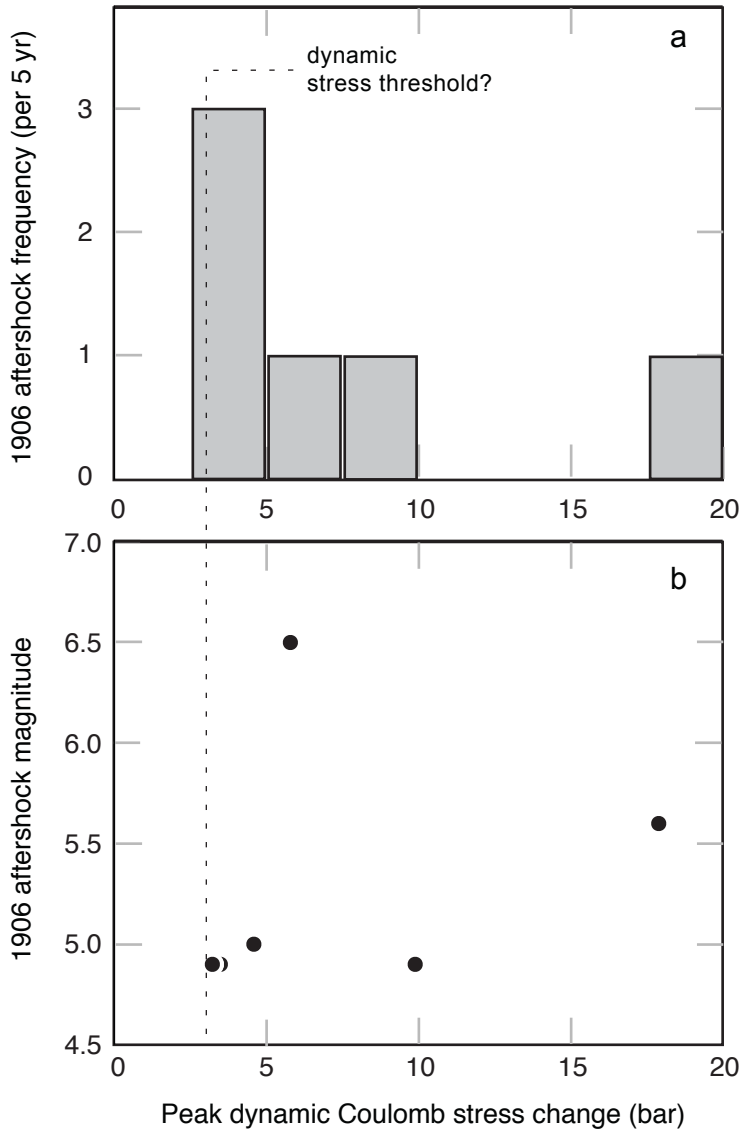

Figure 12. 1906 aftershock frequency (a) and magnitude (b) as a function of calculated peak dynamic Coulomb stress change. 1906 aftershocks from Meltzner and Wald (2003) up through the 1911 event are included; their fault planes are assumed to be parallel to the local strike of the San Andreas fault, with a friction coefficient of 0.6. Because of location uncertainty, the mean stress change within a circle of radius 5 km is used for the calculation. The Song et al (2007) source model for the 1906 earthquake is used. Although no positive correlation is observed in either case, all shocks occurred where the peak dynamic Coulomb stress exceeded 3 bars, perhaps indicative of a threshold for dynamic triggering.

Fig. 12
Doser et al
26 Sep 08